



**HAL**  
open science

# Towards a comprehensive physically-based rainfall-runoff model

Z. Liu, E. Todini

► **To cite this version:**

Z. Liu, E. Todini. Towards a comprehensive physically-based rainfall-runoff model. *Hydrology and Earth System Sciences Discussions*, 2002, 6 (5), pp.859-881. hal-00304733

**HAL Id: hal-00304733**

**<https://hal.science/hal-00304733>**

Submitted on 18 Jun 2008

**HAL** is a multi-disciplinary open access archive for the deposit and dissemination of scientific research documents, whether they are published or not. The documents may come from teaching and research institutions in France or abroad, or from public or private research centers.

L'archive ouverte pluridisciplinaire **HAL**, est destinée au dépôt et à la diffusion de documents scientifiques de niveau recherche, publiés ou non, émanant des établissements d'enseignement et de recherche français ou étrangers, des laboratoires publics ou privés.

# Towards a comprehensive physically-based rainfall-runoff model

Zhiyu Liu and Ezio Todini

Department of Earth and Geo-Environmental Sciences, University of Bologna, Via Zamboni 67, 40127 Bologna, Italy

Email for corresponding author: zhiyu@geomin.unibo.it

## Abstract

This paper introduces TOPKAPI (**TOP**ographic **K**inematic **AP**proximation and **I**ntegration), a new physically-based distributed rainfall-runoff model deriving from the integration in space of the kinematic wave model. The TOPKAPI approach transforms the rainfall-runoff and runoff routing processes into three ‘structurally-similar’ non-linear reservoir differential equations describing different hydrological and hydraulic processes. The geometry of the catchment is described by a lattice of cells over which the equations are integrated to lead to a cascade of non-linear reservoirs. The parameter values of the TOPKAPI model are shown to be scale independent and obtainable from digital elevation maps, soil maps and vegetation or land use maps in terms of slope, soil permeability, roughness and topology. It can be shown, under simplifying assumptions, that the non-linear reservoirs aggregate into three reservoir cascades at the basin scale representing the soil, the surface and the drainage network, following the topographic and geomorphologic elements of the catchment, with parameter values which can be estimated directly from the small scale ones. The main advantage of this approach lies in its capability of being applied at increasing spatial scales without losing model and parameter physical interpretation. The model is foreseen to be suitable for land-use and climate change impact assessment; for extreme flood analysis, given the possibility of its extension to ungauged catchments; and last but not least as a promising tool for use with General Circulation Models (GCMs). To demonstrate the quality of the comprehensive distributed/lumped TOPKAPI approach, this paper presents a case study application to the Upper Reno river basin with an area of 1051 km<sup>2</sup> based on a DEM grid scale of 200 m. In addition, a real-world case of applying the TOPKAPI model to the Arno river basin, with an area of 8135 km<sup>2</sup> and using a DEM grid scale of 1000 m, for the development of the real-time flood forecasting system of the Arno river will be described. The TOPKAPI model results demonstrate good agreement between observed and simulated responses in the two catchments, which encourages further developments of the model.

**Keywords:** rainfall-runoff modelling, topographic, kinematic wave approximation, spatial integration, physical meaning, non-linear reservoir model, distributed and lumped

## Introduction

The study of the impacts of land use and climate changes on the hydrological regimes of river basins requires a better understanding of how climate, topography-geomorphology, soils and vegetation interact to control runoff at the field, hillslope and catchment scales. These interactions can be represented within complex physically-based distributed models (e.g. SHE: Abbott *et al.*, 1986 a,b). But, traditional physically-based distributed models usually work at a small size and require a large amount of data and lengthy computation times which limit their application. Todini (1988) has pointed out that a promising direction in model development is to lump the differential equations at increasing scales except for a few essential parameters and to make them computationally affordable. Although the validity of effective parameter values that must be used with

large scale catchments has been questioned (Beven, 1989), nonetheless a correct integration of the differential equations from the point to the finite dimension of a pixel, and from the pixel to larger scales, can actually generate relatively scale-independent physically-based models, which preserve the physical meaning (although as averages) of the model parameters.

On the basis of a critical analysis of two well known and widely used hydrological rainfall-runoff models - namely the ARNO (Todini, 1996) and the TOPMODEL (Beven and Kirby, 1979; Beven *et al.*, 1984; Sivapalan *et al.*, 1987), Todini (1995) recently proposed the TOPKAPI (**TOP**ographic **K**inematic **AP**proximation and **I**ntegration) model. The ARNO model is a variable contributing area semi-distributed conceptual model controlled by the total soil moisture storage, and widely used for real-time flood

forecasting. The major disadvantage of the ARNO model is the lack of physical grounds for establishing some of the parameters, which reduces its possible extension to ungauged catchments. The TOPMODEL is a variable contributing area model in which the predominant factors determining the formation of runoff are represented by the topography, the transmissivity of the soil and its vertical delay. However, the model preserves its physical meaning only at the hillslope scale (Franchini *et al.*, 1996), while it degrades into a conceptual model at larger scales, with the same problems mentioned for the ARNO model.

In contrast, the TOPKAPI model is based on the lumping of a kinematic wave assumption in the soil, on the surface and in the drainage network, and leads to transforming the rainfall-runoff and runoff routing processes into three non-linear reservoir differential equations which can be solved analytically (Liu, 2002). The geometry of the catchment is described by a lattice of cells (the pixels of a DEM) over which the equations are integrated to lead to a cascade of non-linear reservoirs. The parameter values of the TOPKAPI model are scale independent and obtainable from a digital elevation map, soil map and vegetation or land-use map in terms of slope, soil permeability, roughness and topology. It can be shown, under simplifying assumptions, that the non-linear cascade aggregates into a unique non-linear reservoir at the basin level, with parameter values that can be estimated directly from the small scale ones without losing physical meaning.

The present paper explains the overall structure and methodology of the TOPKAPI model, the non-linear reservoir equation and its solution technique, the data requirements, and the model calibration procedure. To demonstrate the quality of the TOPKAPI approach, a case study of applying the TOPKAPI model to the Upper Reno river basin is presented, to clarify the data and calibration requirements of the model together with the aggregation capabilities when moving from the distributed to the lumped versions of the TOPKAPI model. A real-world case of applying the TOPKAPI model to the Arno river basin, with an area of 8135 km<sup>2</sup> and using a DEM grid scale of 1000 m, for the development of areal-time flood forecasting system for the Arno River is also presented.

## Structure and methodology of the TOPKAPI model

The TOPKAPI is a comprehensive distributed-lumped approach. The distributed TOPKAPI model is used to identify the mechanism governing the dynamics of the saturated area contributing to the surface runoff as a function of the total water storage, thus obtaining a law underpinning

the development of the lumped model.

The model is based on the idea of combining the kinematic approach with the topography of the basin; the latter is described by a Digital Elevation Model (DEM) whose grid size generally increases with the overall dimensions. Each grid cell of the DEM is assigned a value for each of the physical characteristics represented in the model. The flow paths and slopes are evaluated starting from the DEM, according to a neighbourhood relationship based on the principle of minimum energy cost (Band, 1986).

The integration in space of the kinematic wave equations results in three 'structurally-similar' non-linear reservoir equations describing different hydrological and hydraulic processes. This lumping is performed on the individual cell of the DEM in the distributed model, while in the lumped model it is performed at the basin level. The equations obtained for the local scale and for the lumped scale are structurally similar; what distinguishes them are the coefficients, which in one case have local significance and, in the other, summarise the local properties in a global manner.

The present TOPKAPI model (Fig. 1) is structured around five modules that represent the evapotranspiration, snowmelt, soil water, surface water and channel water components respectively. For the deep aquifer flow, the response time caused by the vertical transport of water through the thick soil above this aquifer is so large that horizontal flow in the aquifer can be assumed to be almost constant with no significant response on one specific storm event in a catchment (Todini, 1995). Hence, initially, the model does not account for water percolation towards the deeper subsoil layers and for their contribution to the discharge; this is planned as an additional model layer in a future model development.

The soil water component is affected by subsurface flow (or interflow) in a horizontal direction defined as drainage; drainage occurs in a surface soil layer, of limited thickness and with high hydraulic conductivity due to its macroporosity. The drainage mechanism plays a fundamental role in the model both as a direct contribution to the flow in the drainage network and most of all as a factor regulating the soil water balance, particularly in activating the production of overland flow. The soil water component is the most characterising aspect of the model because it regulates the functioning of the contributing saturated areas. The surface water component is activated on the basis of this mechanism. Lastly, both components contribute to feeding the drainage network.

The most complex and physically realistic model for estimating actual evapotranspiration is the Penman-Monteith equation, which has been widely used in many distributed

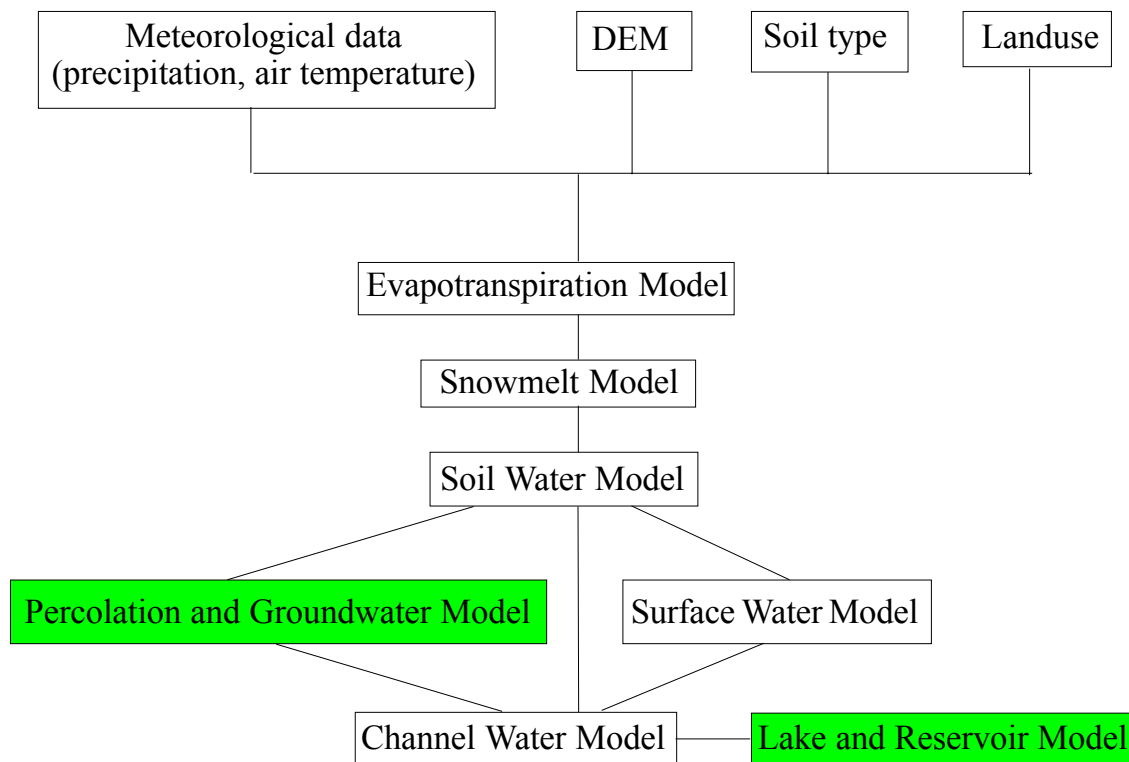


Fig. 1. The components of the TOPKAPI model

models, e.g. SHE (Abbott *et al.*, 1986 a,b), DHSVM (Wigmosta *et al.*, 1994). However, a simplified approach is generally necessary because in many countries the required historical data for Penman-Monteith estimations are not extensively available; and, in addition, apart from a few meteorological stations, almost nowhere are real-time data available for flood forecasting applications. Evapotranspiration plays a major role not only in terms of its instantaneous impact, but in terms of its cumulative temporal effect on the soil moisture volume depletion; this reduces the need for an extremely accurate expression, provided that its integral effect is well preserved. In the present TOPKAPI model, evapotranspiration can be introduced directly as an input to the model or computed externally or estimated internally by a radiation method (Doorembos *et al.*, 1984) starting from the temperature and from other topographic, geographic and climatic information, as described in the ARNO model (Todini, 1996). Again, for reasons of limited data availability, the snow accumulation and melting (snowmelt) component is driven by a radiation estimate based upon the air temperature measurements, which is also borrowed from the ARNO model. In the following sections, the three basic components, the soil water, surface water and channel water will be described in detail.

## The distributed TOPKAPI model

### THE SOIL WATER COMPONENT

#### *Fundamental assumptions*

- (1) Precipitation is constant over the integration domain (namely the single cell), by means of suitable averaging and lumping operations of the local rainfall data, such as Thiessen polygons and Block Kriging (de Marsily, 1986; Matheron, 1970) techniques;
- (2) All of the precipitation falling on the soil infiltrates into it, unless the soil is already saturated in a particular zone; this is equivalent to adopting as the sole mechanism for the formation of overland flow the saturation mechanism from below, (Dunne, 1978);
- (3) The slope of the water table coincides with the slope of the ground, unless the latter is very small (less than 0.01%); this constitutes the fundamental assumption of the approximation of the kinematic wave in the Saint Venant equations, and it implies the adoption of a kinematic wave propagation model with regard to horizontal flow, or drainage, in the unsaturated area (Henderson and Wooding, 1965; Beven, 1981);
- (4) Local transmissivity, like local horizontal flow, depends on the total water content of the soil, i.e. it depends on

the integral of the water content profile in a vertical direction;

- (5) Saturated hydraulic conductivity is constant with depth in a surface soil layer but is much larger than that at deeper layers; this forms the basis for the vertical aggregation of the transmissivity.

**Kinematic wave formulation for sub-surface flow**

In the TOPKAPI model, the horizontal sub-surface flow,  $q$ , is calculated by the approximation Eqn. (1) (Benning, 1994; Todini and Ciarapica, 2001):

$$q = \tan(\beta)k_s L \tilde{\Theta}^\alpha \tag{1}$$

with 
$$\tilde{\Theta} = \frac{1}{L} \int_0^L \tilde{\vartheta}(z) dz = \frac{1}{L} \int_0^L \frac{\vartheta - \vartheta_r}{\vartheta_s - \vartheta_r} dz$$

where  $\beta$  is the slope angle,  $k_s$  is the saturated hydraulic conductivity in  $ms^{-1}$ ,  $L$  is the thickness of the surface soil layer in m,  $\tilde{\Theta}$  is the reduced soil moisture content,  $\vartheta_r$  is the residual soil moisture content,  $\vartheta_s$  is the saturated soil moisture content,  $\vartheta$  is the water content in the soil,  $\tilde{\vartheta}(z)$  is the mean value along the vertical profile of the reduced soil moisture content and  $\alpha$  is a parameter which depends on the soil characteristics (Benning, 1994; Todini, 1995).

Combined with the equation for continuity of mass, the following system is obtained:

$$\begin{cases} (\vartheta_s - \vartheta_r)L \frac{\partial \tilde{\Theta}}{\partial t} + \frac{\partial q}{\partial x} = p \\ q = \tan(\beta)k_s L \tilde{\Theta}^\alpha \end{cases} \tag{2}$$

where  $x$  is the main direction of flow along a cell,  $t$  is the time,  $q$  is the horizontal flow in the soil due to drainage, corresponding to a discharge per unit of width in  $m^2 s^{-1}$ , and  $p$  is the intensity of precipitation in  $m s^{-1}$ . The model is written in just one direction since it is assumed that the flow is characterised by a preferential direction, which can be described as the direction of maximum slope.

Equation (2), rewritten in terms of actual total water content in the soil,  $\eta = (\vartheta_s - \vartheta_r)L \tilde{\Theta}$ , along the vertical profile, with the substitution

$$C = \frac{Lk_s \tan(\beta)}{(\vartheta_s - \vartheta_r)^\alpha L^\alpha} \tag{3}$$

leads to the kinematic equation

$$\frac{\partial \eta}{\partial t} = p - \frac{Lk_s \tan(\beta)}{(\vartheta_s - \vartheta_r)^\alpha L^\alpha} \frac{\partial \eta^\alpha}{\partial x} = p - C \frac{\partial \eta^\alpha}{\partial x} \tag{4}$$

Here, the term  $C$  represents in physical terms a *local conductivity coefficient*, since it depends on soil parameters for a particular position or a particular cell, which encompasses the effects of hydraulic conductivity and slope, to which it is directly proportional, and storage capacity, to which it is inversely proportional.

**Non-linear reservoir model for the soil water in a generic cell**

By integrating Eqn. (4) in the soil over the  $i^{th}$  DEM grid cell, whose space dimension is  $X$ , gives

$$\frac{\partial v_{s_i}}{\partial t} = pX - (C_{s_i} \eta_i^{\alpha_s} - C_{s_{i-1}} \eta_{i-1}^{\alpha_s}) \tag{5}$$

where  $v_{s_i}$  is the volume per unit of width stored in the  $i^{th}$  cell in  $m^2$ , while the last term in Eqn. (5) represents the inflow and outflow balance. A subscript  $s$  is introduced here to distinguish this soil water equation from the ones relevant to the overland and the drainage network flows.

It is quite evident that the coefficients  $C_s$  are no longer the physically measurable quantities, which are defined at a point; rather, they represent integral average values for the entire cell, which nonetheless are still strongly related to the measurable quantities.

In the TOPKAPI model, the grid cells are connected by a tree shaped network; water moves downslope along this tree-shaped flow pathway starting from the initial cells (without upstream contributing areas) representing the ‘sources’, towards the outlet. According to this procedure, and assuming that in each cell the variation of the vertical water content along the cell is negligible, the volume of water stored in each cell (per unit width) can be related to the total water content that is equivalent to the free water volume in depth, by means of the simple expression

$$v_{s_i} = X \eta_i \tag{6}$$

Substituting for  $\eta_i$  in Eqn. (6) and writing it for the ‘source’ cells in each flow pathway, the following non-linear reservoir equation is obtained:

$$\frac{\partial V_{s_i}}{\partial t} = p_i X^2 - \frac{C_{s_i} X}{X^{2\alpha_s}} V_{s_i}^{\alpha_s} \tag{7}$$

Similarly a non-linear reservoir equation can be written for a generic cell, given the total inflow to the cell, such that

$$\frac{\partial V_{s_i}}{\partial t} = (p_i X^2 + Q_{o_i}^u + Q_{s_i}^u) - \frac{C_{s_i} X}{X^{2\alpha_s}} V_{s_i}^{\alpha_s} \tag{8}$$

where  $V_{s_i}$  is the volume stored in the  $i^{\text{th}}$  cell in  $\text{m}^3$ ,  $Q_{o_i}^u$  is the discharge entering the active cell  $i$  as overland flow from the upstream contributing area in  $\text{m}^3 \text{s}^{-1}$ , and  $Q_{s_i}^u$  is the discharge entering the active cell as subsurface flow from the upstream contributing area in  $\text{m}^3 \text{s}^{-1}$ .

### Soil moisture accounting in a grid cell

For the  $i^{\text{th}}$  cell at each time-step, the soil water balance can be calculated as follows:

$$Q_{s_i}^d = (p_i X^2 + Q_{o_i}^u + Q_{s_i}^u) - \frac{V_{s_i}'(t_0 + T) - V_{s_i}(t_0)}{T} \quad (9)$$

$$e_{o_i} = \max\{[V_{s_i}'(t_0 + T) - \min(V_{s_i}'(t_0 + T), V_{s_i}(t_0))], 0\} \quad (10)$$

$$V_{s_i}(t_0 + T) = \min[V_{s_i}'(t_0 + T), V_{sm_i}] - E_a X^2 \quad (11)$$

where  $T$  is the computational time interval in seconds,  $t_0$  is the initial time of the computation step,  $V_{s_i}'(t_0 + T)$  is the solution of Eqn. (8) at the time  $t_0 + T$  in  $\text{m}^3$ ,  $V_{s_i}(t_0)$  is the initial soil water storage in the  $i^{\text{th}}$  cell at the time  $t_0$  in  $\text{m}^3$ ,  $Q_{s_i}^d$  is the outflow discharge from the  $i^{\text{th}}$  cell during the time  $t_0$  to  $t_0 + T$  in  $\text{m}^3 \text{s}^{-1}$ ,  $e_{o_i}$  is the saturation excess volume for the  $i^{\text{th}}$  cell in  $\text{m}^3$ ,  $V_{sm_i}$  is the saturated soil water storage in the  $i^{\text{th}}$  cell in  $\text{m}^3$ ,  $E_a$  is the actual evapotranspiration within the time interval calculated by the evapotranspiration model in  $m$ , and  $V_{s_i}(t_0 + T)$  is the soil water volume stored in the soil in the  $i^{\text{th}}$  cell at time  $t_0 + T$ .

Up to this point it has been implicitly assumed that the entire outflow from a cell flows into the downstream cell immediately. However, this is not entirely true since note has to be taken of the depletion effected by the drainage network. Thus, for the cells in the channel network, the outflow is still evaluated by Eqn. (9), but it is then partitioned between the channel and the downstream cell according to a gradient based upon the average slope of the four surrounding cells. This allows determination of the amount of subsurface flow feeding the drainage channel network. This operation of flow partition is also performed for the overland flow.

### THE SURFACE WATER AND CHANNEL WATER COMPONENTS

The input to the surface water model is the *precipitation excess* resulting from the saturation of the surface soil layer. In addition, the water in the soil can ex-filtrate on the surface as return flow due to a sudden change in hillslope or soil

property, and thus also feeds the overland flow. The subsurface flow and the overland flow together feed the channel along the drainage network.

### Non-linear reservoir model for overland flow and channel flow in a grid cell

Overland flow routing is described similarly to the soil component, according to the kinematic approach (Wooding, 1965) in which the momentum equation is approximated by means of Manning's formula. The kinematic wave approximation for overland flow is described as

$$\begin{cases} \frac{\partial h_o}{\partial t} = r_o - \frac{\partial q_o}{\partial x} \\ q_o = \frac{1}{n_o} (\tan \beta)^{\frac{1}{2}} h_o^{\frac{5}{3}} = C_o h_o^{\alpha_o} \end{cases} \quad (12)$$

where  $h_o$  is the water depth over the ground surface in  $m$ ,  $r_o$  is the saturation excess resulting from the solution of the soil water balance, either as the precipitation excess or the ex-filtration from the soil in absence of rainfall in  $\text{ms}^{-1}$ ,  $n_o$  is the Manning friction coefficient for the surface roughness in  $\text{m}^{-\frac{1}{3}} \text{s}^{-1}$ ,  $C_o = (\tan \beta)^{\frac{1}{2}} / n_o$  is the coefficient relevant to the Manning formula for overland flow, and  $\alpha_o = 5/3$  is the exponent which derives from using the Manning formula. A subscript  $o$  denotes the overland flow.

By analogy with what was done for the soil, assuming that the surface water depth is constant over the cell and integrating the kinematic equation over the longitudinal dimension, gives the non-linear reservoir model for the overland flow for the  $i^{\text{th}}$  cell as

$$\frac{\partial V_{o_i}}{\partial t} = r_{o_i} X^2 - \frac{C_{o_i} X}{X^{2\alpha_o}} V_{o_i}^{\alpha_o} \quad (13)$$

where  $V_{o_i}$  is the surface water volume in the cell in  $\text{m}^3$ .

Similar considerations also apply to the channel network, which is assumed to be tree-shaped with reaches having wide rectangular cross-sections. In this case, the channel surface width is not constant but is assumed to be increasing towards the catchment outlet. Under these assumptions, the non-linear reservoir model can be written for a generic reach as

$$\frac{\partial V_{c_i}}{\partial t} = (r_{c_i} X W_i + Q_{c_i}^u) - \frac{C_{c_i} W_i}{(X W_i)^{\alpha_c}} V_{c_i}^{\alpha_c} \quad (14)$$

where  $V_{c_i}$  is the volume of water stored in the  $i^{\text{th}}$  channel reach in  $\text{m}^3$ ,  $W_i$  is the width of the  $i^{\text{th}}$  rectangular channel reach in  $m$ ,  $Q_{c_i}^u$  is the inflow discharge from the upstream

reaches in  $m^3 s^{-1}$ ,  $r_c$  is the lateral drainage input, including the overland runoff reaching the channel reach and the soil drainage reaching the channel reach in  $m s^{-1}$ ,  $C_c = s_0^{1/2}/n_c$  is the coefficient relevant to the Manning formula for channel flow,  $s_0$  is the bed slope, assumed to be equal to the ground surface slope,  $n_c$  is the Manning friction coefficient for the channel roughness in  $m^{-1/3} s^{-1}$  and  $\alpha_c = 5/3$  is the exponent which derives from using the Manning formula. The channel width  $W_i$  is taken to increase as a function of the area drained by the  $i^{th}$  cell on the basis of geomorphological considerations, such that

$$W_i = W_{max} + \left[ \frac{W_{max} - W_{min}}{\sqrt{A_{tot}} - \sqrt{A_{th}}} \right] \left( \sqrt{A_{dr_i}} - \sqrt{A_{tot}} \right) \quad (15)$$

where  $W_{max}$  is the maximum width, at the basin outlet,  $W_{min}$  is the minimum width, corresponding to the threshold area,  $A_{th}$  is the threshold area which is the minimum upstream drainage area required to initiate a channel,  $A_{tot}$  is the total area and  $A_{dr_i}$  is the area drained by the  $i^{th}$  cell.

#### PHILOSOPHY OF APPLICATION OF THE DISTRIBUTED TOPKAPI MODEL

##### ***Solution technique for the non-linear reservoir equation***

The TOPKAPI formulation leads to three non-linear reservoir equations describing the subsurface flow, the overland flow and the channel flow. In the first version of the TOPKAPI model (Todini and Ciarapica, 2001), the solution of the non-linear reservoir equation was based upon a variable step fifth order Runge-Kutta numerical algorithm due to Cash and Karp (1990). Nowadays, the authors have found that the non-linear reservoir equation can be solved analytically based on an appropriate approximation (Liu, 2002), providing a more efficient scheme in terms of running time. Details of analytical solutions based on appropriate approximations are given in Appendix A.

##### ***Data requirements and parameters***

The TOPKAPI model requires terrain data (e.g. from DTM or DEM land survey), soil survey and vegetation or land-use, as well as geographical co-ordinates and measurements of precipitation, evapotranspiration or air temperature.

As far as the parameters are concerned, there are seven classes of parameters in the TOPKAPI model, namely  $L$  (thickness of the surface soil layer in m),  $k_s$  (saturated hydraulic conductivity in  $m s^{-1}$ ),  $\vartheta_r$  (residual soil moisture content),  $\vartheta_s$  (saturated soil moisture content),  $a_s$  (exponent

of the transmissivity law for the soil component, assumed to be constant for all the cells),  $n_o$  (surface roughness in  $m^{-1/3} s^{-1}$ ), and  $n_c$  (roughness for the channel in  $m^{-1/3} s^{-1}$ ). Five of the parameters ( $L$ ,  $k_s$ ,  $\vartheta_r$ ,  $\vartheta_s$  and  $a_s$ ) relate to the soil and control runoff production, whilst the other two ( $n_o$ ,  $n_c$ ) are routing parameters.

##### ***DEM application in the TOPKAPI model***

The DEM application consists of: identifying and correcting sinks and false outlets, identifying the connections among the cells thereby giving the flow pathways, calculating the steepness, and cumulating the drained area for the automatic detection of the drainage network. Utilities serving these purposes are provided in GRASS (Geographic Resources Analysis Support System), but unfortunately they are not suitable for application to the TOPKAPI model because they are based on neighbourhood functions that use a moving  $3 \times 3$  point spatial window, where the elevation of the central point is compared with the heights of the eight connected neighbours. For the TOPKAPI model, or in general for any model using a finite difference approach, in the moving  $3 \times 3$  point spatial window the four neighbouring cells adjacent to each corner have to be neglected, which means physically that drainage is only possible to the north, east, south or west for the four adjacent cells at each edge.

##### ***Model calibration***

The TOPKAPI model is considered as a physically based model, with all parameters having physical meanings which can be measured directly through fieldwork. Although it is physically based, the model still needs calibration because of the uncertainty of the information on the topography, soil characteristics and land cover. Nonetheless the calibration of the TOPKAPI parameters is more an adjustment than a conventional calibration and is carried out by a simple trial-and-error method.

In the TOPKAPI model, the initial soil saturation condition can be set as follows. First, the initial soil saturation percentage is set as the same value (e.g. 0.5) for all cells according to a dry situation at the beginning of the calibration period. Then the TOPKAPI program is run to obtain the soil saturation condition at a chosen time when the soil is supposed to be in the same state as the initial condition. This procedure gives realistic values for the initial condition, particularly with regard to the spatial distribution of the saturation percentage. At the initial condition, it is also assumed that there is no snow or surface water over the slopes and the water depth in a generic channel cell increases as a linear function of the channel width of the cell.

Model parameter values are assigned according to the type of soil, land cover and channel order by the method of Strahler (1957). The initial parameter values can be taken from the literature, e.g. the values of the soil parameters  $k_s$ ,  $\vartheta_r$  and  $\vartheta_s$  can be taken from the USDA parameters for the infiltration model of Green-Ampt. Initial values for parameters  $n_o$  and  $n_c$  can be estimated by referring to Tables 5.5 and 5.6 in the book on *Open Channel Hydraulics* by Chow (1959) and the report on *Roughness Characteristics of Natural Channels* by Barnes (1967), while  $a_s$  usually varies 2.0 ~ 4.0 based on the soil property. In general, the ranges of the values of the model parameter are:  $L=0.10 \sim 2.00$  m,  $k_s=10^{-6} \sim 10^{-3}$  m s<sup>-1</sup>,  $\vartheta_s=0.25 \sim 0.70$ ,  $\vartheta_r=0.01 \sim 0.10$ ,  $n_o=0.05 \sim 0.40$  m<sup>-1/3</sup> s<sup>-1</sup>,  $n_c=0.02 \sim 0.08$  m<sup>-1/3</sup> s<sup>-1</sup>.

## The lumped TOPKAPI model

### DESCRIPTION OF THE LUMPED TOPKAPI MODEL

The overall structure of the lumped TOPKAPI model is shown schematically in Fig. 2. A catchment is regarded as a dynamic system composed of three reservoirs: the soil

reservoir, the surface reservoir and the channel reservoir. In the flow simulation, on the basis of the soil condition and actual evapotranspiration, the precipitation in the catchment is partitioned into direct runoff and infiltration using the Beta-distribution curve, which reflects the non-linear relationship between the soil water storage and the saturated contributing area in the basin. The infiltration and direct runoff are input into the soil reservoir and surface reservoir, respectively. Outflows from the two reservoirs as interflow and overland flow are then drained into the channel reservoir to form the channel flow.

As mentioned before, the TOPKAPI approach is a comprehensive distributed-lumped approach. Theoretically it proves that the lumped version of the TOPKAPI model can be derived directly from the results of the distributed version and does not require additional calibration.

In order to obtain the lumped version of the TOPKAPI, the point kinematic wave equation is integrated over the entire system of cells describing the basin. This is done first by computing the total volume stored in the soil, on the surface or in the channel network by adding up the single cell volumes as a function of the geomorphology and

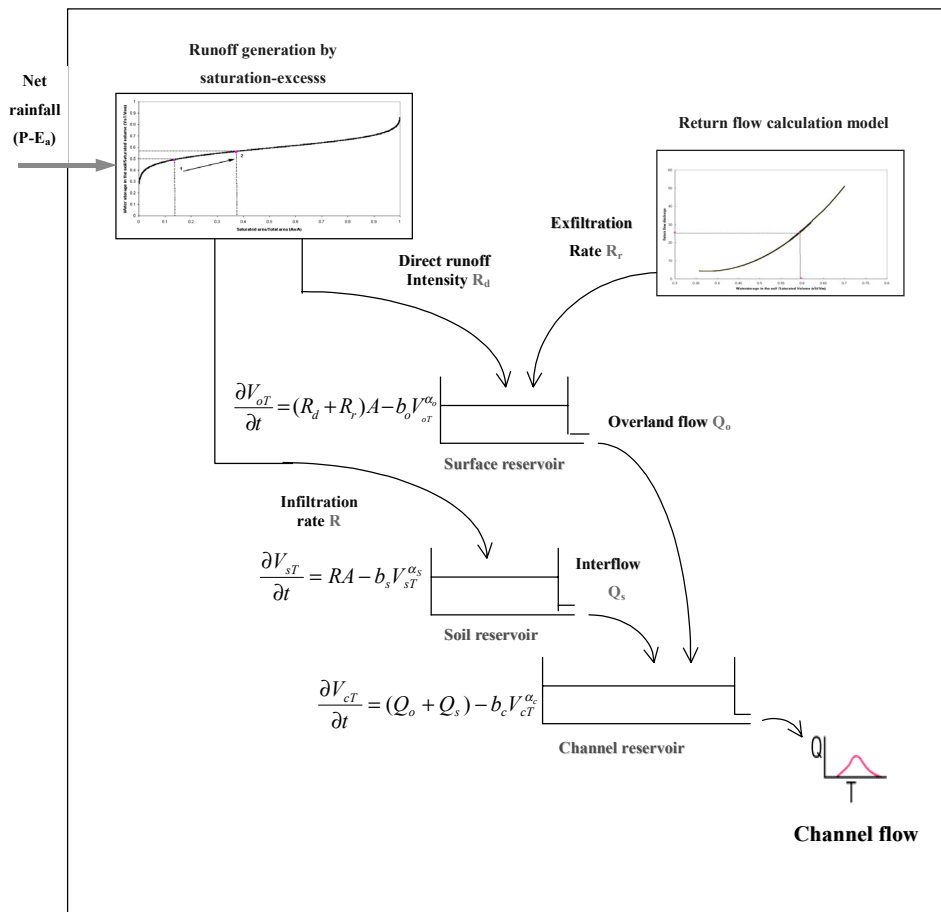


Fig. 2. Structure of the lumped TOPKAPI model



topology of the catchment. Under the assumption that the difference between the inflow to a cell and the time variation of the water storage do not vary significantly in space, this integration and aggregation results in a non-linear reservoir equation for representing the basin as a whole of the form (Todini and Ciarapica, 2001; Liu, 2002).

$$\frac{\partial V_{sT}}{\partial t} = RA - \left( \frac{\alpha_s + 1}{\alpha_s X} \frac{1}{\left[ \sum_{l=1}^{N-1} \left( \prod_{m=l}^{N-1} f_m \right) + 1 \right]} \right)^{\alpha_s} X \bar{C}_{sT} V_{sT}^{\alpha_s} = RA - b_s V_{sT}^{\alpha_s} \quad (16)$$

with

$$\bar{C}_{sT} = \left\{ \sum_{i=1}^N \left[ \frac{1 + \sum_{l=1}^{j-1} \left( \prod_{m=l}^{j-1} f_m \right)}{1 + \sum_{l=1}^{N-1} \left( \prod_{m=l}^{N-1} f_m \right)} \right]^{\frac{\alpha_s+1}{\alpha_s}} - \left[ \frac{\sum_{l=1}^{j-1} \left( \prod_{m=l}^{j-1} f_m \right)}{1 + \sum_{l=1}^{N-1} \left( \prod_{m=l}^{N-1} f_m \right)} \right]^{\frac{\alpha_s+1}{\alpha_s}} \right\} / C_{s_i}^{1/\alpha_s}$$

where  $i$  is the index of a generic cell,  $j$  is the index of cells drained by the  $i^{th}$  cell,  $N$  is the total number of cells in the upstream contributing area,  $V_{sT}$  is the water storage in the catchment in  $m^3$ ,  $R$  is the infiltration rate in  $m s^{-1}$ ,  $A$  is the catchment area,  $C_{s_i}$  is the local conveyance for the  $i^{th}$  cell,  $f_m$  represents the fraction of the total outflow from the  $m^{th}$  cell which flows towards the downstream cell,  $\alpha_s$  is a soil model parameter assumed constant in the catchment, and  $b_s$  is a lumped soil reservoir parameter which incorporates in an aggregated way the topography and physical properties of the soil.

Equation (16) corresponds to a non-linear reservoir model and represents the lumped dynamics of the water stored in the soil. The same type of equation can be written for the overland flow and for the drainage network, thus transforming the distributed TOPKAPI model into a lumped model characterised by three ‘structurally similar’ non-linear reservoirs, namely ‘soil reservoir’, ‘surface reservoir’ and ‘channel reservoir’.

The infiltration rate term in Eqn. (16) must be evaluated by separating precipitation into direct runoff and infiltration into the soil. In order to obtain this separation, a relationship between the extent of saturated areas and the volume stored

in the catchment is introduced, similar to what is done in the Xinanjiang model (Zhao, 1977), in the Probability Distributed Model (Moore and Clarke, 1981; Moore, 1985, 1999) and in the ARNO model (Todini, 1996). Given the availability of the distributed TOPKAPI version, this relationship can be obtained by means of extensive simulation. At each time step the number of saturated cells is compared to the total volume of water stored in the soil over the entire catchment. Denoting total water storage in the soil by  $V_{sT}$ , the soil water storage at the total saturation condition by  $V_{ss}$ , and the total saturation area by  $A_s$ , the relationship between the extent of saturated areas and the volume stored in the catchment can be approximated by a Beta-distribution function curve expressed by:

$$\frac{A_s}{A} = \int_0^{\frac{V_{sT}}{V_{ss}}} \frac{\Gamma(r+s)}{\Gamma(r)\Gamma(s)} \varphi^{r-1} (1-\varphi)^{s-1} d\varphi \quad (17)$$

where  $\Gamma(\cdot)$  is the Gamma function, and  $r$  and  $s$  two parameters of the Beta-distribution curve.

### Surface runoff calculation

Surface runoff is the sum of direct runoff and the return flow caused by ex-filtration. In the lumped TOPKAPI model, the Beta-distribution function curve as expressed by Eqn. (17) is thus used to compute, in the lumped form, the overall inflow as infiltration  $R$  to the soil reservoir and the overall saturation excess as direct runoff  $R_d$  ( $m s^{-1}$ ) entered into the surface reservoir by the following equation:

$$R_d = P - \left( \frac{V_{sT_2}}{V_{ss}} - \frac{V_{sT_1}}{V_{ss}} \right) \frac{V_{ss}}{A(t_2 - t_1)} \quad (18)$$

where  $V_{sT_1}$ ,  $V_{sT_2}$  represent the soil water storage in the catchment at time  $t_1$ , and  $t_2 = t_1 + \Delta t$  respectively where  $\Delta t$  is the computation time interval, and  $P$  represents the catchment average net precipitation intensity ( $m s^{-1}$ ).

The soil water can ex-filtrate to generate the return flow. In the present TOPKAPI model, the return flow is estimated based on a limiting parabolic curve representing the relationship between the return flow discharge and the fraction of water storage in the catchment, which is estimated based on the points from the distributed TOPKAPI model. This parabolic curve can be expressed as:

$$R_r = Q_{return} / A = \frac{a_1}{A} \left( \frac{\bar{V}_{sT}}{V_{ss}} \right)^2 + \frac{a_2}{A} \frac{\bar{V}_{sT}}{V_{ss}} + \frac{a_3}{A} \quad (19)$$

where  $R_r$  is the return flow ex-filtration rate,  $Q_{return}$  is the calculated return flow discharge on the surface during the time interval  $t_1 \sim t_2$ ,  $\bar{V}_{sT} = 0.5(V_{sT_1} + V_{sT_2})$  is the averaged soil water storage in  $m^3$ , and  $a_1$ ,  $a_2$  and  $a_3$  are parameters estimated on the basis of the points from the distributed TOPKAPI model.

Accordingly, the infiltration rate into the soil within the time interval  $Dt$  can be computed by:

$$R = \left( \frac{V_{sT_2}}{V_{ss}} - \frac{V_{sT_1}}{V_{ss}} \right) \frac{V_{ss}}{A(t_2 - t_1)} - \frac{Q_{return}}{A} \quad (20)$$

The quantities  $R$  and  $R_d$  plus  $R_r$  are then input to the soil reservoir and the surface reservoir, respectively (see Fig. 3). The interflow and overland flow can be obtained by computing the water balance, and are then together drained into the channel reservoir to generate the total outflow at the basin outlet.

## Fields of application

Since its advent in 1995, the TOPKAPI model has been applied to several catchments for different uses such as flood forecasting, extreme flood analysis, and predicting hydrological response under changed landscape conditions caused by human activities. The distributed version of the TOPKAPI model allows for its calibration on the basis of physical considerations and, in particular, its extension to ungauged catchments. The lumped version of the TOPKAPI model allows for the extensive simulations needed when used in combination with a stochastic rainfall generator for deriving, through continuous simulation, extreme discharges and flood wave volumes.

The model has been applied to the upper Reno river basin (1051 km<sup>2</sup>) (Todini and Ciarapica, 2001) and the Arno river basin (8135 km<sup>2</sup>) for flood forecasting (Liu, 2002), and to the Magra catchment (1682 km<sup>2</sup>) for extreme flood analysis (Liu and Todini, 2000). The DEM grid size employed

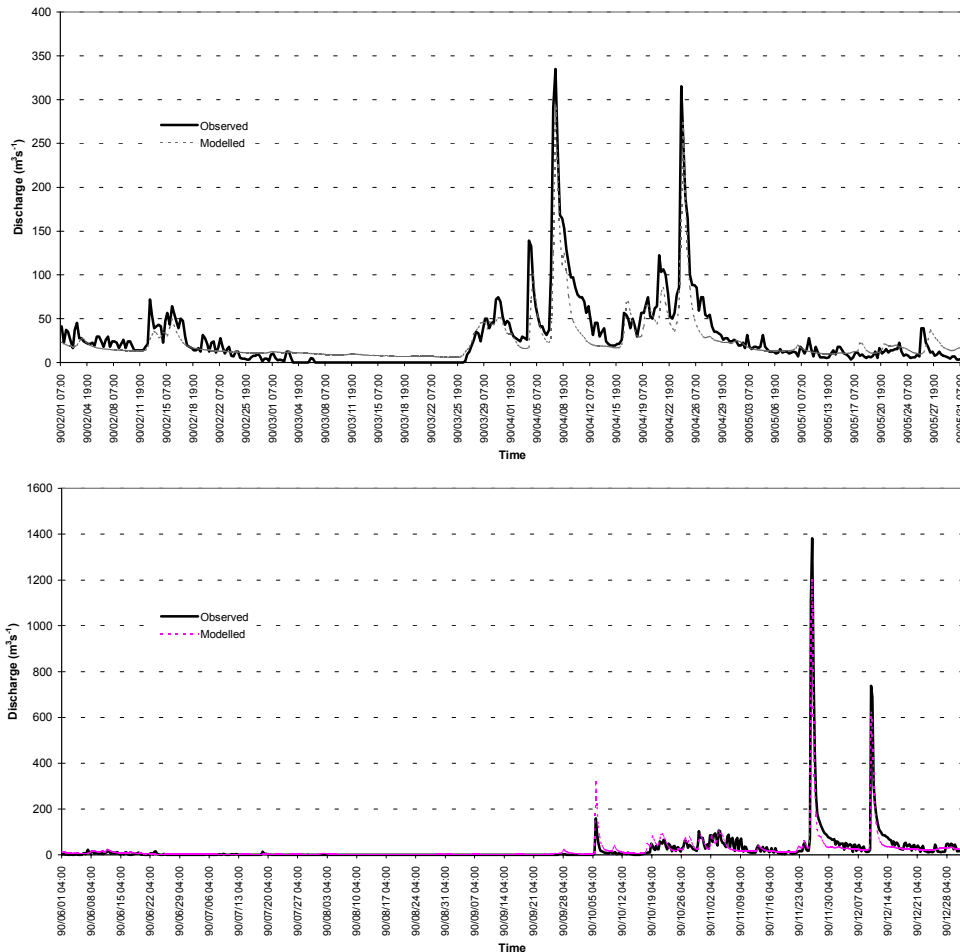


Fig. 3. TOPKAPI model results in the Upper Reno catchment: (a) small flood events, (b) major flood events

increases with the catchment size, ranging from 200 m to 1 km for these three examples.

A case study applying both the distributed and lumped TOPKAPI model to the upper Reno river basin and including the distributed TOPKAPI model for developing a real-time flood forecasting system for the Arno River is presented here in detail.

## The Upper Reno river basin case study

### CATCHMENT CHARACTERISTICS

#### Topography

The Reno River in Italy rises on the northern slopes of the Apennines and flows inside the Emilia-Romagna region (Fig. 4a) with a total watercourse of 210 km. The basin has a surface area of 4930 km<sup>2</sup> and a variation in height above sea level of up to 2,000 m (see Fig. 4b). The upper part of the basin is gauged at Casalecchio on the outskirts of the city of Bologna, and drains an area of approximately 1051 km<sup>2</sup> within which it reaches its maximum elevation of 2000 m. A digital elevation model (DEM) on a 400 × 400 m

grid is available for most of the Upper Reno river basin falling under the Emilia Romagna Regional Authority.

#### Soils

The Upper Reno river basin comprises primarily clayey and marly soil, as well as alluvial deposits in its lower section (see Fig. 4c and Table 1).

Table 1. Soil types in the Upper Reno river basin(Fig. 3c)

| Class | Soil Types   |
|-------|--|
| a     | Arenaceous turbidites, calcarenites                                    |
| b     | Arenaceous turbidites, marly limestone turbidites                      |
| c     | Marly arenaceous turbidites  |
| d     | Arenaceous turbidites  |
| e     | Marly limestone and calcarenite turbidites, clays and marly limestones |
| f     | Clays, sands and conglomerates   |
| g     | Alluvial deposits  |

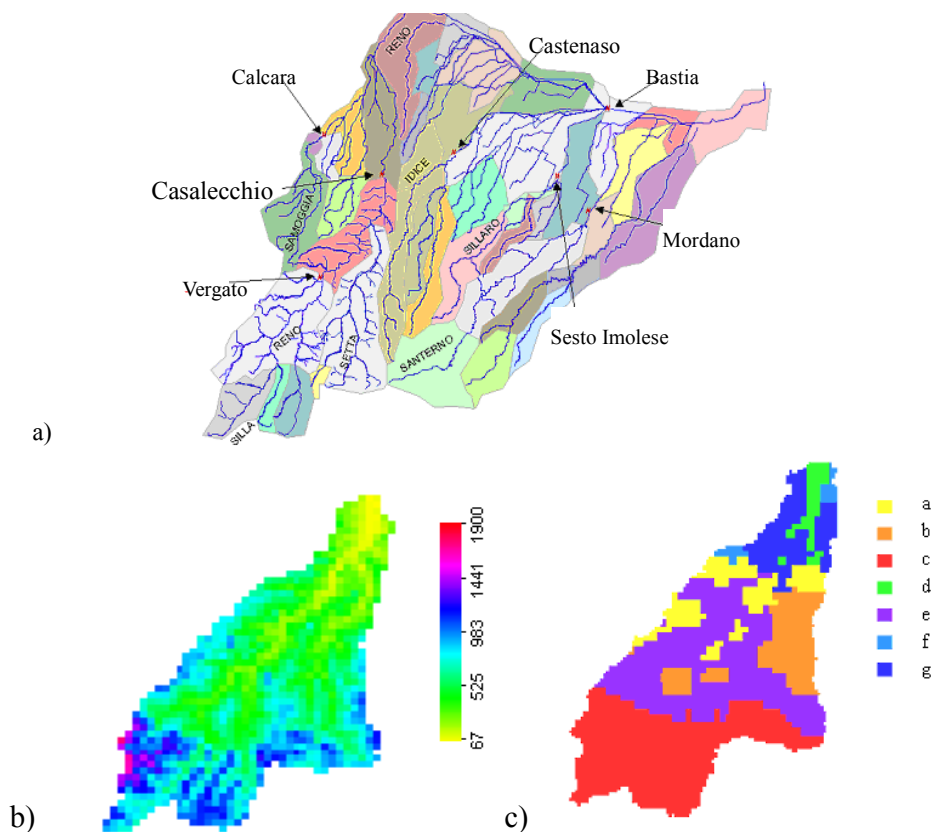


Fig. 4. Reno river basin: a) Reno river system, sub-basins and water level stations, b) DEM map for the Upper Reno catchment (legend: elevation above sea level in meter), c) Soil type map for the Upper Reno catchment

### Vegetation and land use

Vegetation on the highest parts of the Apennines is made up of herbaceous formations and blueberry derived from cultivation and grazing which were once particularly intensive. The most widespread land use in the strip of territory along the Reno, both for the lowland area as well as for the mountain area, is agriculture, except for the impracticable areas at high levels and those areas subject to periodical flooding.

#### MODEL CALIBRATION OF THE DISTRIBUTED TOPKAPI MODEL

##### Hydrometeorological data availability

The hydrological dataset in the year 1990 is selected for calibration in the Upper Reno river basin, since in this year, from 24 to 26 November, 1990, a relatively large flood event with a peak discharge of  $1317 \text{ m}^3 \text{ s}^{-1}$  occurred. Hourly measurements from 24 raingauges and 10 thermometers were available while discharges were computed from hourly levels by means of a well-verified rating curve available for Casalecchio. The areal rainfall distribution was estimated by the Thiessen Polygon method.

##### Model calibration

The model calibration was performed at a 1-hour time-step using the hydrological dataset of 1990. An initial estimate for the model parameter set was derived using the available broad descriptions of soil types given in Table 1 and Strahler channel order, together with values taken from the literature. Adjustment of parameters was performed manually and, at the end, the values given in Table 2 were retained. The model results are shown in Fig. 3, and the model efficiencies are: 0.850 ( $R^2$ : the proportion of the variance in the observations

accounted for by the model), 0.843 ( $r^2$ : the coefficient of determination) and 0.918 ( $r$ : the correlation coefficient), respectively.

#### DERIVATION OF THE LUMPED TOPKAPI MODEL PARAMETERS AND MODEL APPLICATION

As explained previously, the lumped TOPKAPI model can be derived directly from the distributed results of the distributed TOPKAPI model. Given the availability of the distributed TOPKAPI version, at each step in time the number of saturated cells is compared with the total volume of water stored in the soil over the entire catchment. The relationship between the extent of saturated areas and the volume stored in the catchment can be approximated by a Beta-distribution function curve which is shown in Fig. 5.

In addition, the distributed TOPKAPI model showed that the overland flow comprises two parts, one from direct runoff in the saturated area and the other from return flow which is the ex-filtration of soil water into the surface. In the Upper Reno river basin, the maximum discharge value of the return flow was  $43 \text{ m}^3 \text{ s}^{-1}$ . Hence, the generation of return flow is very significant in the catchment, and therefore should be simulated in the lumped TOPKAPI model. Figure 6 shows the relationship between the return flow discharge and the soil water storage in the catchment, and its approximation by the limiting parabolic curve adopted in the lumped TOPKAPI model.

The parameters of the lumped TOPKAPI model are listed in Table 3 and simulation results are shown in Figs. 7 and 8. Figure 7 compares the runoff calculated by the distributed TOPKAPI model with that obtained using the lumped model, while Fig. 8 shows the comparison of the observed discharges at Casalecchio and those computed using the distributed and lumped TOPKAPI model. The lumped TOPKAPI model performance measures are as high as the distributed ones, namely  $R^2 = 0.887$ ,  $r^2 = 0.867$  and  $r = 0.931$ .

Table 2. Calibration parameters for the different soil classes, land uses and channel orders

| Soil Class | $\vartheta_s - \vartheta_r$ | $\alpha$ | $k_s$<br>( $\text{m s}^{-1}$ ) | $L$ (m) | Soil use class | $n_o$<br>( $\text{m}^{-1/3} \text{ s}^{-1}$ ) | Strahler channel order | $n_c$<br>( $\text{m}^{-1/3} \text{ s}^{-1}$ ) |
|------------|-----------------------------|----------|--------------------------------|---------|----------------|---|------------------------|---|
| a          | 0.36                        | 2.5      | 2.50E-04                       | 1.65    | a              | 0.085   | I                      | 0.045   |
| b          | 0.36                        | 2.5      | 2.20E-04                       | 1.60    | b              | 0.085   | II                     | 0.040   |
| c          | 0.36                        | 2.5      | 1.50E-04                       | 0.30    | c              | 0.090   | III                    | 0.035   |
| d          | 0.36                        | 2.5      | 2.30E-04                       | 1.50    | d              | 0.085   | IV                     | 0.035   |
| e          | 0.30                        | 2.5      | 9.00E-04                       | 1.75    | e              | 0.080   |                        |   |
| f          | 0.60                        | 2.5      | 1.20E-03                       | 2.75    | f              | 0.080   |                        |   |
| g          | 0.64                        | 2.5      | 1.40E-03                       | 3.50    | g              | 0.080   |                        |   |

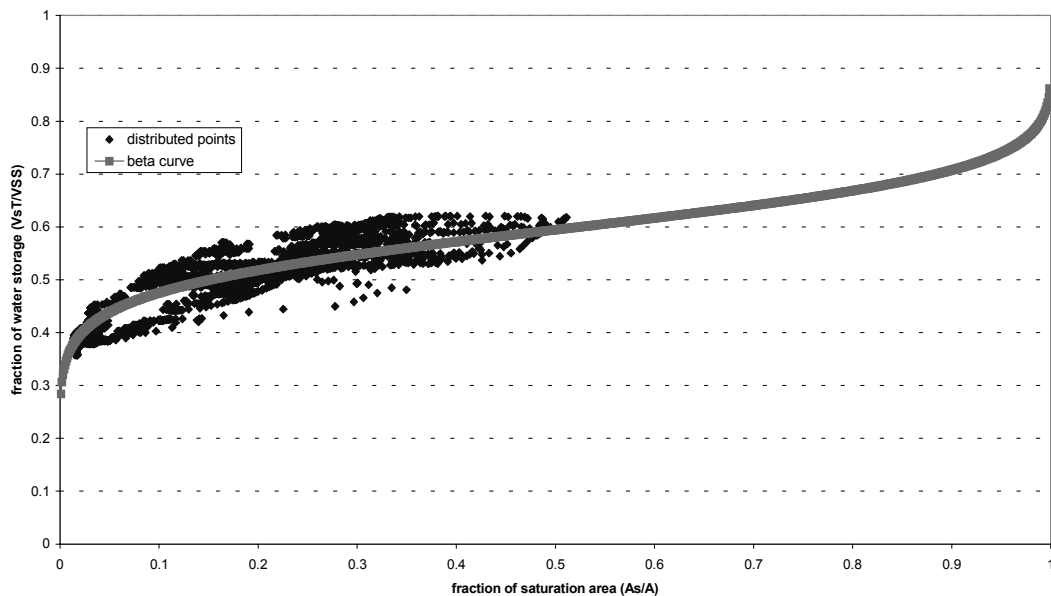


Fig. 5. The Beta-distribution function fitted to the distributed TOPKAPI simulated results ( $r=0.11, s=0.16$ )

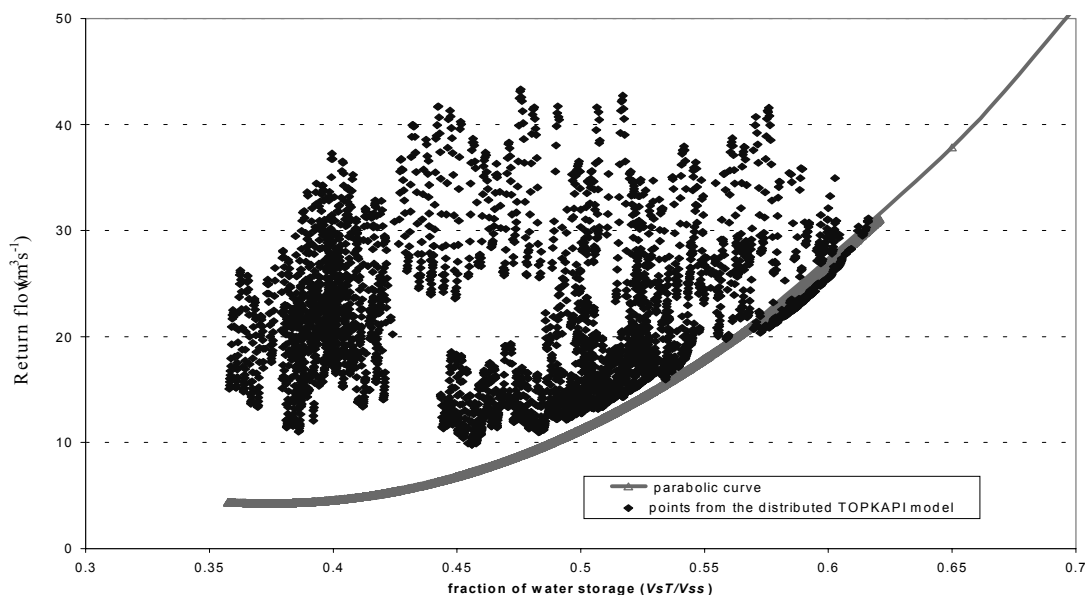


Fig. 6. A limiting parabolic curve used for calculating the return flow from the soil water storage in the catchment

$$Q_{return} = a_1 \left( \frac{\bar{V}_{sT}}{V_{ss}} \right)^2 + a_2 \frac{\bar{V}_{sT}}{V_{ss}} + a_3 \quad \text{with } a_1=441, a_2=-330, a_3=66.$$

Table 3. Lumped TOPKAPI model parameters used in the Upper Reno river basin

| Three non-linear reservoirs |               |               | Beta-distribution function<br>(used for calculating direct runoff) |      | Parabolic curve function<br>(used for calculating return flow) |       |       |
|-----------------------------|---------------|---------------|--|------|--|-------|-------|
| Soil $b_s$                  | Surface $b_o$ | Channel $b_c$ | $r$  | $s$  | $a_1$  | $a_2$ | $a_3$ |
| 7.98E-022                   | 6.10E-010     | 7.35E-010     | 0.11   | 0.16 | 441.   | -330. | 66.0  |

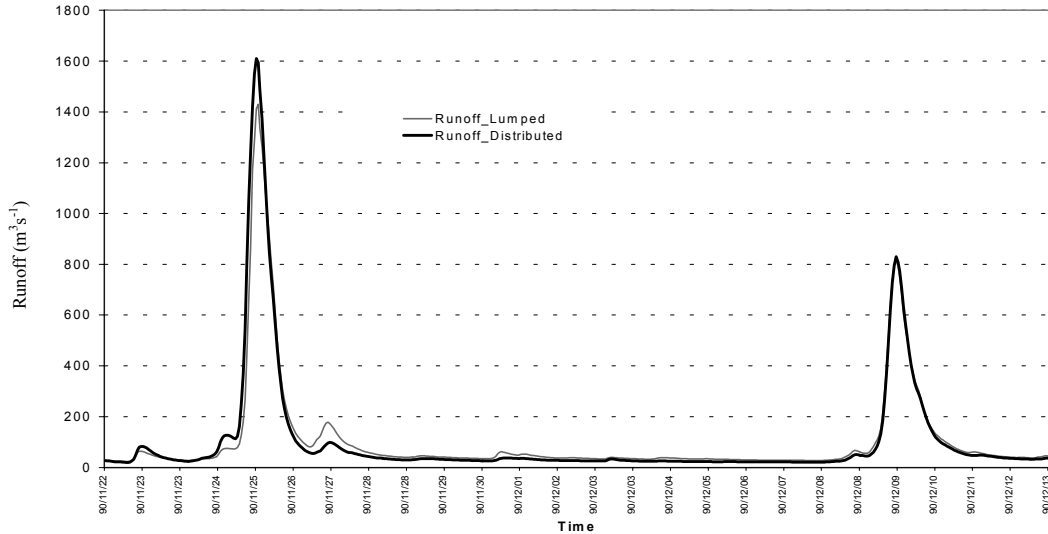


Fig. 7. Comparison of calculated runoff using the distributed and lumped TOPKAPI models for the Upper Reno catchment. Thick solid line: distributed model, thin solid line: lumped model. Major flood events.

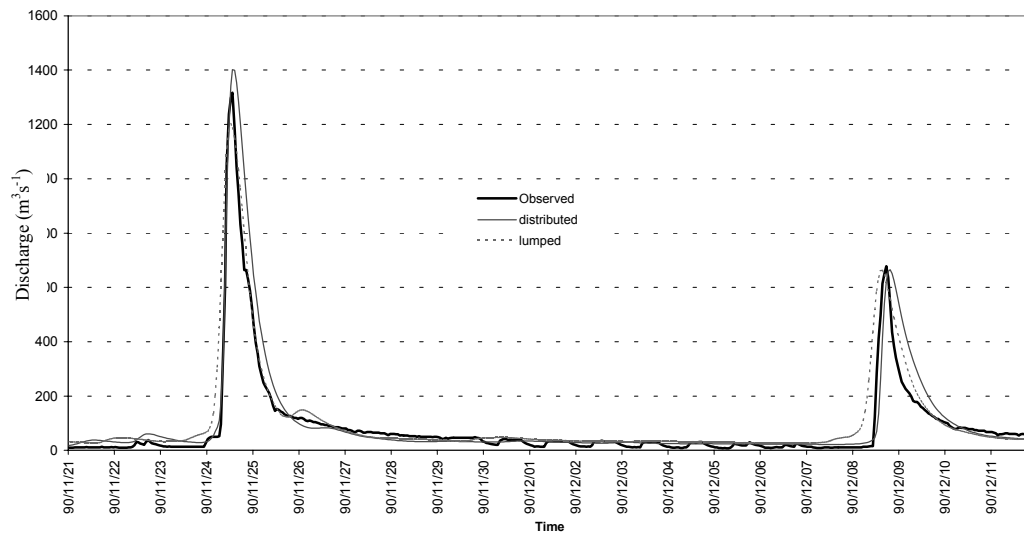


Fig. 8. Comparison of observed and modelled discharges for the Reno at Casalecchio. Thick solid line: observed; thin solid line: distributed model; dash line: lumped model. Major flood events.

### Discussion of results

Figure 6 shows only marginal differences between the simulated runoff (i.e. the total drainage into the channel) for the whole river basin and for the discharge at Casavecchio, generated by the distributed TOPKAPI model and the lumped model, are practically identical with only marginal differences. This is despite the first one being computed by integrating a cascade of 6325 non-linear reservoirs representing the soil, the overland flow and non-linear reservoirs representing the channel flow, whilst the second one is computed using the Beta-distribution function curve given by Eqn. (17) and a return-flow estimation curve

given by Eqn. (19), plus one soil reservoir simulating the interflow (see Fig. 2), one surface reservoir simulating the overland flow and one channel reservoir simulating the channel flow, with an enormous reduction in computer time.

This case study demonstrates that the lumped version of the TOPKAPI model is already suitable for reproducing the overall runoff that reaches the river network generated by the distributed model. As far as the drainage network component is concerned, the lumped model produces a flood wave generally anticipated with respect to the distributed one (see Fig. 8), especially for the low flow period, which is consistent with the non-linear behaviour of unsteady flow with travel times reducing with the dimension of the event.

The TOPKAPI approach is attractive in that it is a comprehensive distributed/lumped approach in which the lumped model parameters are estimated directly from the distributed model without calibration.

In this study, it was recognised that the phenomenon of return flow identified in the distributed model must also be considered in the lumped model. Figures 9 and 10 show the comparison of the simulation results obtained by the lumped TOPKAPI model with and without consideration of return flow. If the return flow was not considered in the lumped model, the dynamics of the soil water storage and the calculated discharges would be significantly different from those generated by the distributed model.

## The Arno river basin case study

### RIVER BASIN CHARACTERISTICS

The Arno river basin (Fig. 11a) drains an area of 8228 km<sup>2</sup>, rising in the mountain Falterona (1654 m a.s.l) situated in the northern border of Casentino. The river flows in a south-west to north-east direction to the confluence with the Sieve river (836 km<sup>2</sup>) where it flows east to west to the river mouth. Over its course, the Arno river is joined by major tributaries including the Greve river, Pesa stream, Elsa river and Era river on the left side, and the Bisenzio river and Omrone river on the right side. The watercourse of the river has a total length of approximately 245 km. Local climatic

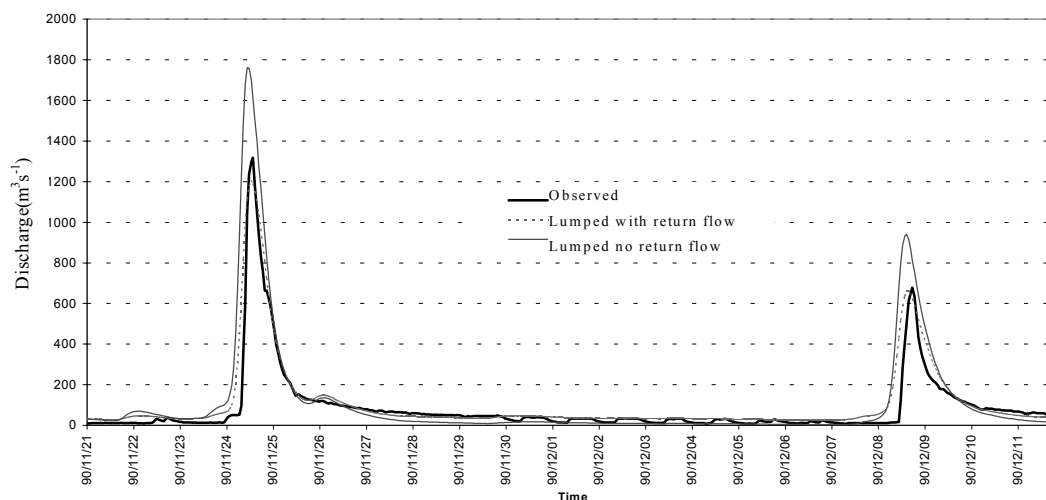


Fig. 9. Comparison of observed and modelled discharges for Casalecchio. Thick solid line: observed; dash line: lumped model with return flow; thin solid line: lumped model without consideration of return flow. Major flood events.



Fig. 10. Comparison of modelled soil water storage in the Upper Reno catchment. Solid line: distributed model; thin solid line: lumped model with return flow; dash line: lumped model without consideration of return flow.

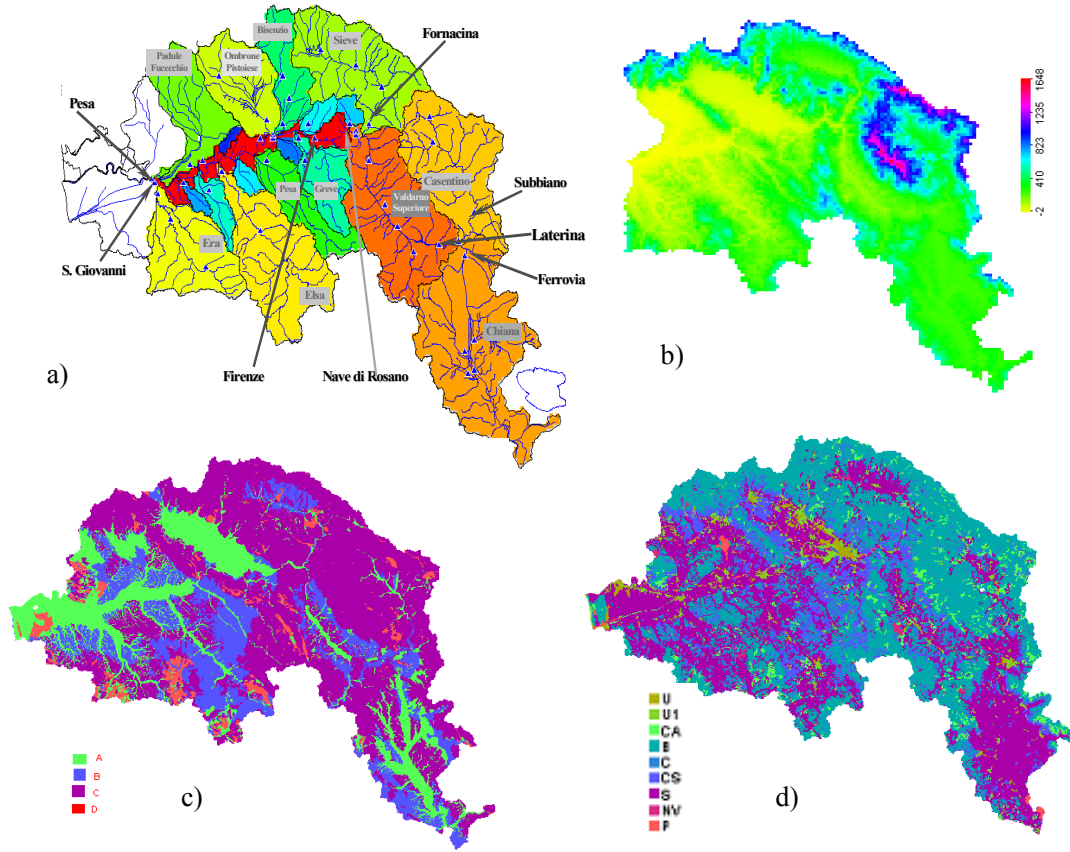


Fig. 11. Arno river basin: (a) river system, sub-basins and water level stations, (b) DEM map (legend: elevation above sea level in meter), (c) Soil type map, and (d) Land use map

tendencies produce the highest flooding risk in the period from September to January when winds from the south-west dominate.

### Topography

The highest areas are found in the mountains of Falterona and Pratomagno in the Casentino (Fig. 11b). The mean elevation of the whole river basin is 292 m a.s. l.. A DEM

data file with a grid scale of 200 m is available for the Arno river basin. In this study, the DEM is used with a grid size of 1km (see Fig. 11b).

### Soils

Based on the SCS classification (Soil Conservation Service, 1972), a soil property map (see Fig. 11c and Table 4) is available giving hydrological soil types. For the whole

Table 4. Legend for pedological data (soil hydrological types)

| No. | Hydrological type of soil (S.C.S/C.N.) | DESCRIPTION   |
|-----|--|---|
| 1   | A                                      | With limited runoff potentiality. Contains deep sands with a very little lime and clay, and deep gravel of high permeability.   |
| 2   | B                                      | With moderately low runoff potentiality. Contains the major part of the sandy soil that is less deep than the one in the group A, but the group as a whole has a high infiltration capacity even when saturated.  |
| 3   | C                                      | With moderately high runoff potentiality. Contains thin soils having a considerable quantity of clay and colloidal material, while less than group D. The group has limited infiltration capacity when saturated. |
| 4   | D                                      | With middle high runoff potentiality. Contains the major part of the clay soil with a high capacity for expanding, but also the thin soils almost impermeable near the surface.                                   |



basin, the major soil type is C, which comprises 57.9 % of the total area. This implies that more than half of the soils possess the hydrological characteristics of a thin soil layer with moderately-high runoff potential, containing a considerable quantity of clay and colloidal material, with limited infiltration capacity when saturated. Also, the soils are thin and of lower permeability in the mountain areas, while the soils in low-lying areas are thick and of moderately high permeability.

### *Vegetation and land use*

The primary land uses in this catchment (see Table 5) are the classes of **B** (38.6%) and **S** (34.7%). In the mountain areas, most land use comprises shrub, undergrowth and overgrowth bush, while in the low-lying areas most land is suitable for arable farming.

Table 5. Legend for land use data

| No. | Class    | Description  |
|-----|----------|--|
| 1   | U        | Urban areas with continuous tissue                   |
| 2   | U1       | Discontinuous urban areas                            |
| 3   | CA       | Forest and arboreal vegetation                       |
| 4   | <b>B</b> | Vegetation of shrub, undergrowth and overgrowth bush |
| 5   | C        | Herbaceous vegetation, meadow-pasture                |
| 6   | CS       | Special cultivated areas, olive, vineyard            |
| 7   | <b>S</b> | Suitable for sowing                                  |
| 8   | NV       | Areas without vegetation                             |
| 9   | P        | Humid areas  |

## APPLICATION OF THE DISTRIBUTED TOPKAPI MODEL

### *Data availability*

Floods have been experienced in 1992, 1993 and 2000. It was decided to choose 1992 as a flood year for model calibration, and use the dataset for 2000 for model verification. Since most raingauges were concentrated in the Upper Firenze in 1992, it was decided to calibrate the TOPKAPI model only in the catchment to Firenze with an area of about 4325 km<sup>2</sup>.

Hourly measurements from 59 raingauges and 7 temperature stations are available for 1992 and 2000, while the discharges of 5 stations — namely Fornacina (Sieve), Subbiano (Casentino), Ponte della Ferrovia (Chiana), Nave

di Rosano (Valdarno Superiore) and Firenze (Arno River) — are computed from hourly river levels by means of well-verified rating curves. The areal rainfall distribution was estimated using the Thiessen Polygon method.

### *Calibration of the TOPKAPI model*

The model calibration was performed at a 1-hour time-step using the hydrological dataset of 1 July to 31 December 1992. The initial parameter values of the three basic components in the TOPKAPI model, the soil water, surface water and channel water components, were estimated from the literature (e.g. using the USDA parameter tables for the Green-Ampt infiltration model). The final parameter values were obtained by ‘trial and error’ on the basis of curve fitting.

Figures 12 to 16 show the comparison of the observed discharges and those computed at Firenze, Nave di Rosano, Fornacina, Subbiano and Ponte della Ferrovia, respectively, using the distributed TOPKAPI model. The model calibration performance statistics and the parameter values are listed in Table 6 and Table 7, respectively.

### *Validation of the TOPKAPI model*

Using the parameter values of Table 7, simulations were carried out using the dataset for the period from 1 July to 31 December 2000. Comparison of observed and simulated hydrographs for the five stations is shown in Figs. 17 to 21. The model simulation performance statistics are shown in Table 8.

### *Discussion of results*

Figures 12 to 21 demonstrate that the distributed TOPKAPI model (based on a DEM with a large grid size of 1000 m) performed well in simulating the floods in the Arno river basin. It did not simulate well the low flows mainly due to the absence of groundwater and lake/reservoir components in the present model. The oscillations at low flows shown in Figs. 12, 13, 17 and 18 for Firenze and Nave di Rosano reflect the effect of a reservoir located at Laterina (see Fig. 11).

Tables 6 and 8 show that the model performance in terms of the coefficient of determination ( $r^2$ ) in the validation period is lower than that in the calibration period, especially for Fornacina and Subbiano. This is very probably due to the poor quality of the measured water levels at the stations of Fornacina and Subbiano. For event 2 (11 July 2000) the measurements for Fornacina are significantly in error, because its peak is higher than the corresponding peaks at

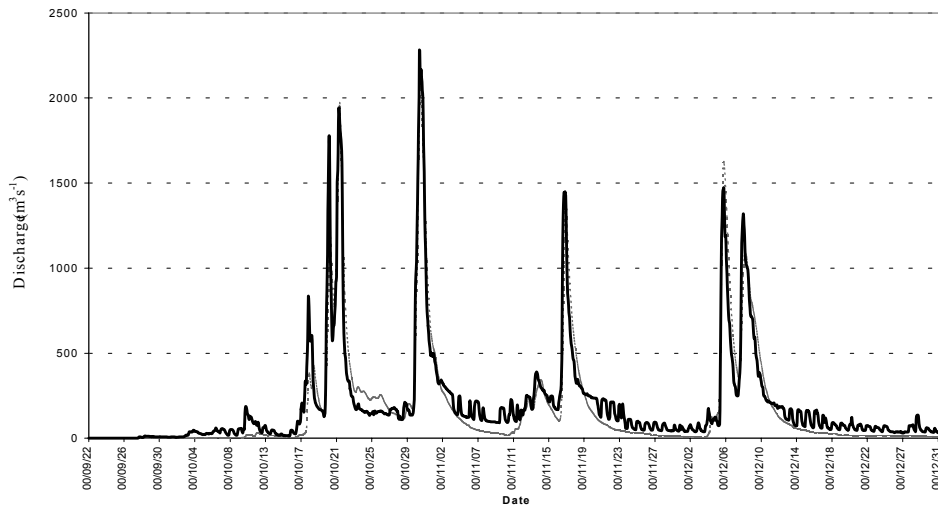


Fig. 12. Model calibration results compared with observed discharges at Firenze. Solid line: observed; Dash line: calculated. Major flood events.

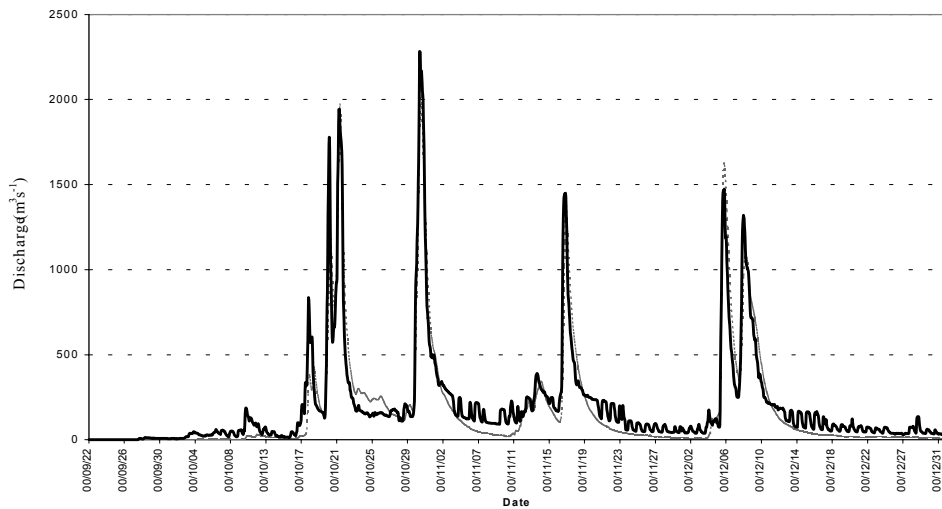


Fig. 13. Model calibration results compared with observed discharges at Nave di Rosano.

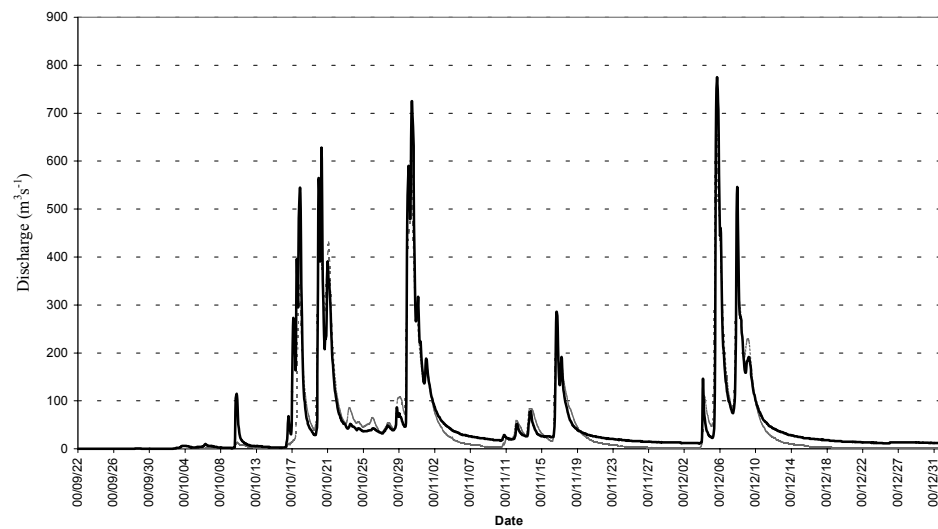


Fig. 14. Model calibration results compared with observed discharges at Fornacina.

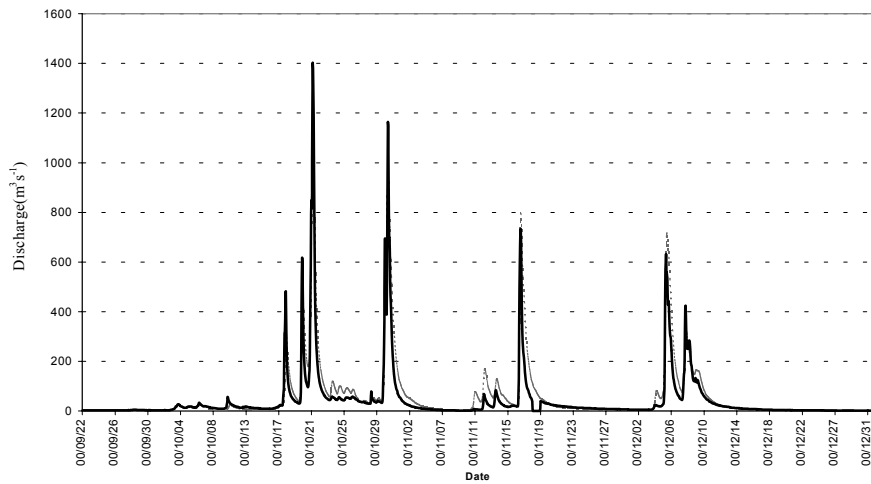


Fig. 15. Model calibration results compared with observed discharges at Subbiano.

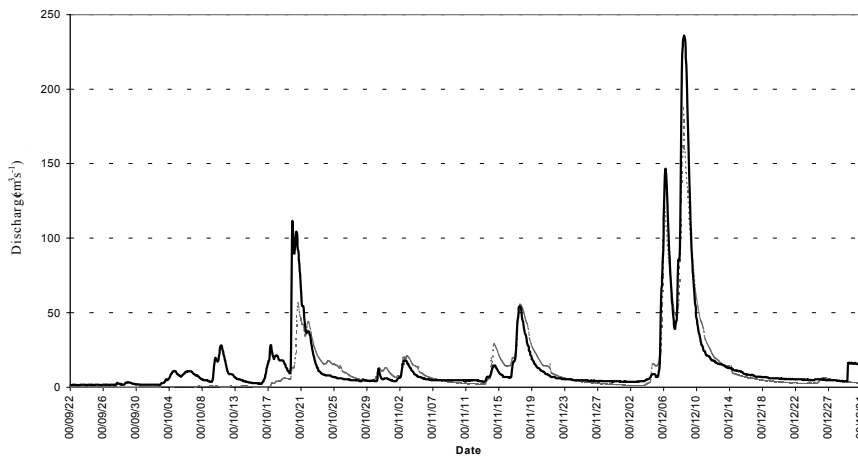


Fig. 16. Model calibration results compared with observed discharges at Ponte di Ferrovia.

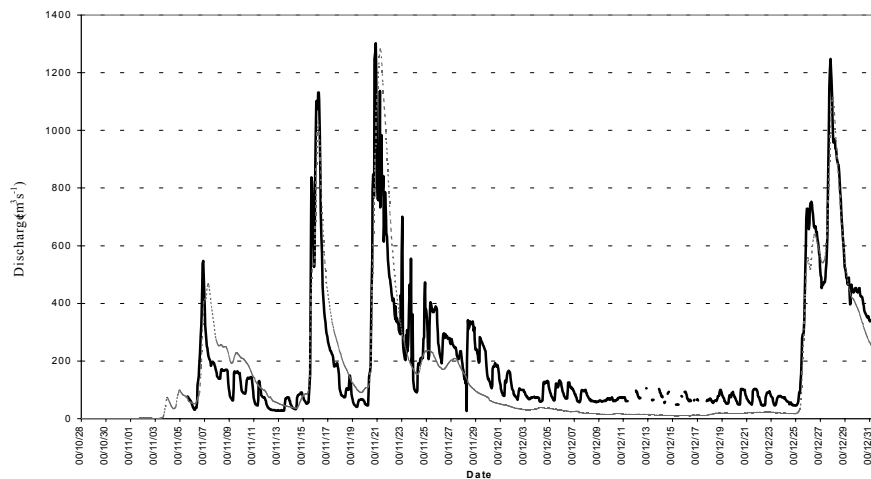


Fig. 17. Model validation results compared with observed discharges at Firenze. Solid line: observed; Dash line: calculated. Major flood events.

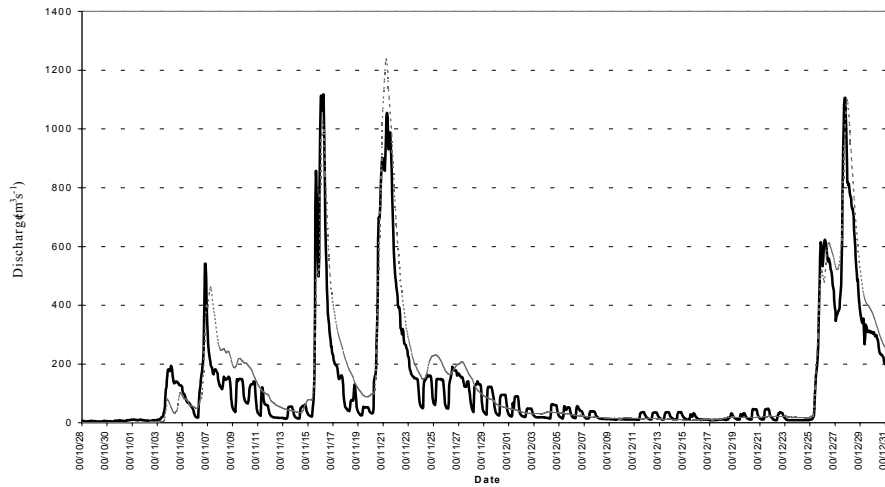


Fig. 18. Model validation results compared with observed discharges at Nave di Rosano.

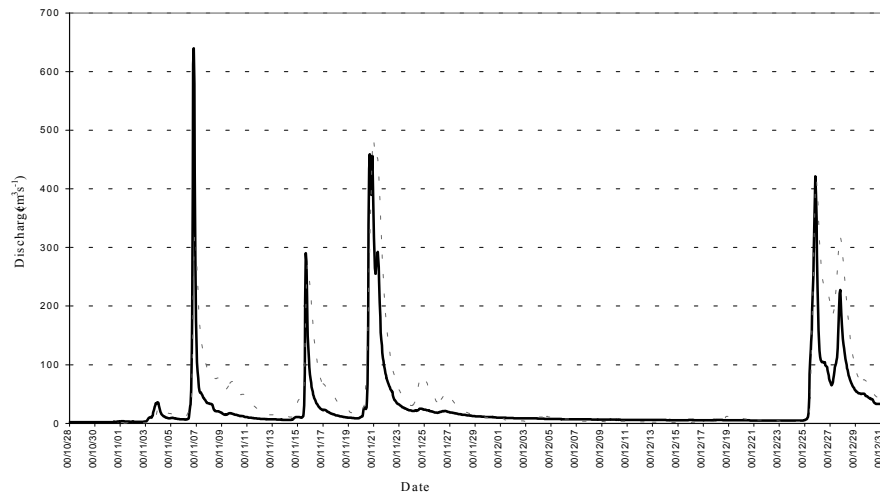


Fig. 19. Model validation results compared with observed discharges at Fornacina.

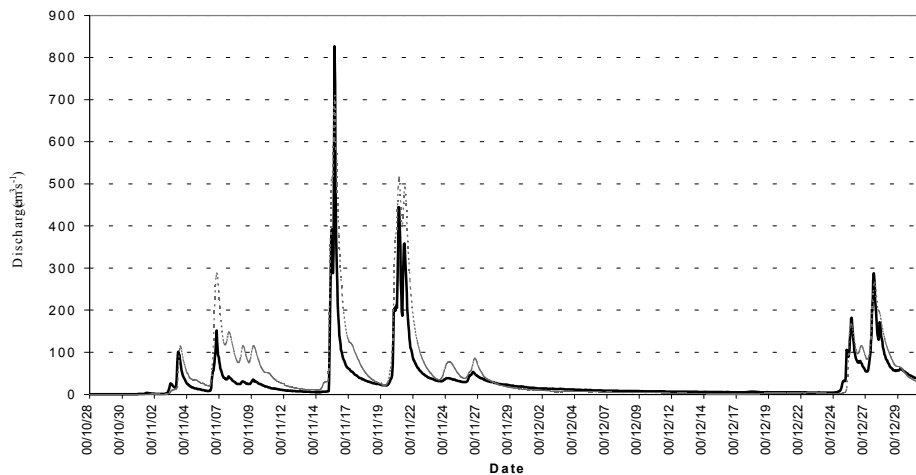


Fig. 20. Model validation results compared with observed discharges at Subbiano.

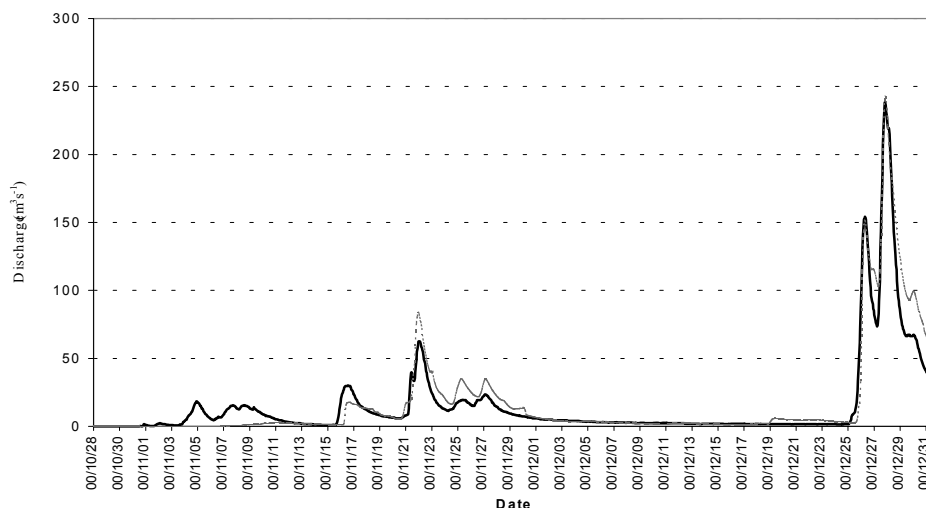


Fig. 21. Model validation results compared with observed discharges at Ponte di Ferrovia.

Table 6. TOPKAPI model calibration statistics in the Upper Firenze catchment in 1992

| Station<br>Performance<br>statistics | Fornacina | Subbiano | Ponte delle<br>Ferrovia | Nave di<br>Rosano | Firenze |
|--------------------------------------|-----------|----------|-------------------------|-------------------|---------|
| $R^2$                                | 0.875     | 0.845    | 0.855                   | 0.915             | 0.916   |
| $r^2$                                | 0.873     | 0.837    | 0.847                   | 0.912             | 0.910   |
| $r$                                  | 0.934     | 0.915    | 0.920                   | 0.955             | 0.954   |

Table 7. Calibration parameters for the different soil classes, land uses and channel orders

| Soil<br>class | $\vartheta_s - \vartheta_r$ | $\alpha$ | $k_s$<br>( $m\ s^{-1}$ ) | $L$<br>( $m$ ) | Land use<br>class | $n_o$<br>( $m^{-1/3}\ s^{-1}$ ) | Strahler<br>channel order | $n_c$<br>( $m^{-1/3}\ s^{-1}$ ) |
|---------------|-----------------------------|----------|--------------------------|----------------|-------------------|---------------------------------|---------------------------|---------------------------------|
| A             | 0.500                       | 2.5      | 6.54E-04                 | 1.20           | U                 | 0.060                           | I                         | 0.045                           |
| B             | 0.535                       | 2.5      | 6.06E-05                 | 0.90           | U1                | 0.100                           | II                        | 0.040                           |
| C             | 0.425                       | 2.5      | 1.89E-05                 | 0.60           | CA                | 0.200                           | III                       | 0.035                           |
| D             | 0.417                       | 2.5      | 1.67E-06                 | 0.30           | <b>B</b>          | 0.150                           | IV                        | 0.030                           |
|               |                             |          |                          |                | C                 | 0.100                           | V                         | 0.025                           |
|               |                             |          |                          |                | CS                | 0.090                           |                           |                                 |
|               |                             |          |                          |                | <b>S</b>          | 0.150                           |                           |                                 |
|               |                             |          |                          |                | NV                | 0.100                           |                           |                                 |
|               |                             |          |                          |                | P                 | 0.010                           |                           |                                 |

Table 8. TOPKAPI model validation performance statistics for the Upper Firenze catchment in 2000

| Station<br>Performance statistics | Fornacina | Subbiano | Ponte delle<br>Ferrovia | Nave di<br>Rosano | Firenze |
|-----------------------------------|-----------|----------|-------------------------|-------------------|---------|
| $R^2$                             | 0.739     | 0.626    | 0.820                   | 0.891             | 0.878   |
| $r^2$                             | 0.732     | 0.608    | 0.811                   | 0.889             | 0.858   |
| $r$                               | 0.856     | 0.780    | 0.901                   | 0.943             | 0.926   |

Nave di Rosano and Firenze (see Figs. 19, 17 and 18), which is generally impossible. Based on the measurements from 1 July to 31 December 2000, the runoff coefficient for Subbiano is calculated to be 0.36 which is lower than its general value (greater than 0.50).

## Conclusions and suggestions

A correct integration of the differential equations from the point to the finite dimension of a pixel, and from the pixel to larger scales, can actually generate relatively scale independent models, which preserve, as averages, the physical meaning of the model parameters. This consideration is reflected in the TOPKAPI approach. The TOPKAPI model couples the kinematic approach with the topography of the catchment and transfers the rainfall-runoff processes into three 'structurally-similar' non-linear reservoir equations describing different hydrological and hydraulic processes. The parameter values of the TOPKAPI model are shown to be scale independent and obtainable from digital elevation maps (e.g. DTM, DEM), soil maps and vegetation or land-use maps in terms of slope, soil permeability, roughness and topography.

The TOPKAPI approach is a comprehensive distributed-lumped one. The distributed TOPKAPI is used to identify the mechanism governing the dynamics of the saturated area contributing to the surface runoff as a function of the total water storage. Theoretically it proves the lumped version of the TOPKAPI model can be derived directly from the distributed version and does not require additional calibration.

With the advantage of being a physically-based model with a simple and parsimonious parameterisation, the TOPKAPI model can have numerous applications ranging from flood forecasting, extreme flood analysis and predicting hydrological response under the changed landscape conditions caused by human activities. Finally, there exists an attractive possibility of deriving model representations from world  $1 \times 1 \text{ km}^2$  cartography (such as for instance GTOPO30 produced by the USGS) to be lumped at the  $50 \times 50$  or  $20 \times 20 \text{ km}^2$  meshes of the Mesoscale or Limited Area Meteorological (LAM) Models the better to reproduce the soil atmosphere exchanges.

The distributed version of the TOPKAPI model allows for its calibration on the basis of physical considerations and, in particular, its extension to ungauged catchments. The lumped version of the TOPKAPI model allows for the extensive simulations needed when used in combination with a stochastic rainfall generator for deriving, through continuous simulation, extreme discharges and flood wave volumes.

The two applications of the TOPKAPI model to the Upper Reno catchment and the Arno River basin demonstrate that the model performs well in simulating floods, although low flows are not as well simulated. The model runs efficiently in terms of calibrating and running time. For the Arno River basin with 8315 cells, only 9 minutes are needed to run a 1-year period with input data sampled at 1 hour. The two applications also show that the model structure is simple and reasonable in simulating the hydrological and hydraulic processes in a basin by using the non-linear reservoir approximation.

Percolation to deeper soil layers has still to be introduced; this was ignored in the initial stage since it was not important in the basins to which the model was originally applied. This objective may be pursued through the introduction of a second soil layer with different characteristics from the upper layer, and involving water movement in a vertical direction feeding into the aquifer. In addition, an approach for incorporating lakes and reservoirs should be included in further developments of the TOPKAPI model.

## References

- Abbott, M.B., Bathurst, J.C., Cunge, J.A., O'Connell, P.E. and Rasmussen, J., 1986a. An introduction to the European Hydrological system – Système Hydrologique Européen, SHE, 1: History and philosophy of a physically based distributed modelling system. *J. Hydrol.*, **87**, 45–59.
- Abbott, M.B., Bathurst, J.C., Cunge, J.A., O'Connell, P.E. and Rasmussen, J., 1986b. An introduction to the European Hydrological system – Système Hydrologique Européen, SHE, 2: Structure of a physically based distributed modelling system. *J. Hydrol.*, **87**, 61–77.
- Band, L.E., 1986. Topographic partition of watersheds with digital elevation models. *Water Resour. Res.*, **22**, 15–24.
- Barnes, H.H., 1967. *Roughness characteristics of natural channels*. United States Government Printing Office, Washington.
- Benning, R.G., 1994. *Towards a new lumped parameterisation at catchment scale*. Master Thesis, University of Wageningen, The Netherlands. 10–45.
- Beven, K.J., 1981. Kinematic subsurface stormflow. *Water Resour. Res.*, **17**, 1419–1424.
- Beven, K.J., 1989. Changing ideas in hydrology – The case of physically based models. *J. Hydrology*, **105**, 157–172.
- Beven, K.J. and Kirkby, M.J., 1979. A physically based, variable contributing area model of basin hydrology. *Hydrol. Sci. Bull.*, **24**, 1–3.
- Beven, K.J., Kirkby, M.J., Schofield, N. and Tagg, A.F., 1984. Testing a physically-based flood forecasting model (TOPMODEL) for three U.K. catchments. *J. Hydrol.*, **69**, 119–143.
- Cash, J.R. and Karp, A. H., 1990. A variable order Runge-Kutta method for initial value problems with rapidly varying right hand sides. *ACM Trans. Math. Software*, **16**, 201–222.
- Chow, V.T., 1959. *Open-Channel Hydraulics*. International student edition. McGraw-Hill.
- Chow, V.T., Maidment, D.R., and Mays, L.W. 1988. *Applied Hydrology*. McGraw-Hill.

- de Marsily, G., 1986. Geostatistic and stochastic approach in hydrogeology. Chapter 11 in *Quantitative hydrology: Groundwater Hydrology for Engineers*. Academic Press, Inc., California. 286–329.
- Doorembos, J., Pruitt, W.O., Aboukhaled, A., Damagnez, J., Dastane, N.G., van den Berg, C., Rijtema, P.E., Ashford, O.M. and Frere, M., 1984. Guidelines for predicting crop water requirements. *FAO Irrig. Drainage Pap.*, 24.
- Dunne, T., 1978. Field studies of hillslope flow process. In: *Hillslope Hydrology* M.J. Kirkby (Ed.). Wiley, New York. 227–293.
- Franchini, M., Wendling, J., Obled, C. and Todini, E., 1996. Physical interpretation and sensitivity analysis of the TOPMODEL. *J. Hydrol.*, **175**, 293–338.
- Henderson, F.M. and Wooding, R.A., 1964. Overland flow and groundwater flow from a steady rainfall of finite duration. *J. Geophys. Res.*, **69**, 1531–1540.
- Liu, Z., 2002. *Toward A Comprehensive Distributed/Lumped Rainfall-Runoff Model: Analysis of Available Physically-Based Models and Proposal of a New TOPKAPI Model*. Ph.D. dissertation, University of Bologna.
- Liu, Z. and Todini, E., 2000. *Application of TOPKAPI Model for Extreme Flood Frequency Analysis Study in Magra Catchment. Hydro-Geological Disasters Reduction: Recent Developments And Perspectives*, Proc. Int. IDNDR Symposium held in Perugia in July.
- Matheron, G., 1970. La théorie des variables régionalisées et ses applications. *Cah. Cent. Morphol. Math.*, **5**.
- Moore, R.J. and Clarke, R.T., 1981. A distribution function approach to rainfall runoff modelling. *Water Resour. Res.*, **17**, 1367–1382.
- Moore, R.J., 1985. The probability-distributed principle and runoff production at point and basin scales. *Hydrol. Sci.*, **30**, 273–297.
- Moore, R.J., 1999. Real-time flood forecasting system: perspectives and prospects, In: *Flood and landslides: Integrated risk assessment*, R. Casal R. and C. Margottini (Eds.). Springer. 147–189.
- O'Callaghan, J.F. and Mark, D.M. 1984. The extraction of drainage networks from digital elevation data. *Computer Vision, Graphics, and Image Processing*, **28**, 323–344.
- Sivapalan, M., Beven, K.J. and Wood, E.F., 1987. On hydrological similarity 2. A scaled model of storm runoff production. *Water Resour. Res.*, **23**, 2266–2278.
- Soil Conservation Service, 1972. *National Engineering Handbook, Section 4. Hydrology*. U.S. Department of Agriculture, Washington D.C.
- Strahler, A.N., 1957. Quantitative analysis of watershed geomorphology. *Trans. Amer. Geophys. Union*, **38**, 913–920.
- Todini, E., 1988. Rainfall-runoff modelling – past, present and future. *J. Hydrol.*, **100**, 341–352.
- Todini, E., 1995. New trends in modeling soil processes from hillslope to GCMS Scales - The role of water and the hydrological cycle in global change, H.R. Oliver and S.A. Oliver (Eds.). NATO ASI Series I: Global Environmental Change, **31**, 317–347.
- Todini, E., 1996. The ARNO rainfall-runoff model. *J. Hydrol.*, **175**, 339–382.
- Todini, E. and Ciarapica, L., 2001. The TOPKAPI model. Chapter 12 in *Mathematical Models of Large Watershed Hydrology*, V.P. Singh et al. (Eds.). Water Resources Publications, Littleton, Colorado.
- Wigmosta, M.S., Vail, L.W. and Lettenmier, D.P., 1994. A distributed hydrology-vegetation model for complex terrain. *Water Resour. Res.*, **30**, 1165–1679.
- Wooding, R.A., 1965. A hydraulic modeling of the catchment-stream problem. 1. Kinematic wave theory. *J. Hydrol.*, **3**, 254–267.
- Zhao, R.J., 1977. *Flood forecasting method for humid regions of China*. East China College of Hydraulic Engineering, Nanjing.

## Appendix

### ANALYTICAL SOLUTION TECHNIQUE FOR THE NON-LINEAR RESERVOIR EQUATION

A general form of the non-linear reservoir equations in the TOPKAPI model can be written as:

$$\frac{dy}{dt} = a - by^c \quad (\text{A.1})$$

where  $y$  is a state variable (e.g. the average soil moisture content, soil water volume in the reservoir, or water depth over the slopes, or in the channel);  $a$ ,  $b$  and  $c$  are constants ( $a$  may be equal zero) in each time-step.

According to the following three different cases:

(a)  $a = 0$ ; (b)  $a \neq 0$ ,  $1 \leq c \leq 2$ ; and (c)  $a \neq 0$ ,  $c > 2$ , different techniques are used for solving the non-linear reservoir equation.

(a)  $a = 0$ . In this case, Eqn. (A.1) can be simplified to:

$$\frac{dy}{dt} = -by^c \quad (\text{A.2})$$

The solution to the above equation can be obtained directly by:

$$y_t = [y_0^{1-c} + b(c-1)(t-t_0)]^{\frac{1}{1-c}} \quad (\text{A.3})$$

where  $y_t$  is the  $y$  at time  $t$ ,  $y_0$  and  $t_0$  are the initial values of  $y$  and  $t$  at each time step.

(b)  $a \neq 0$ ,  $1 \leq c \leq 2$  (e.g.  $c = 5/3$  for the overland flow and channel flow equations of the TOPKAPI model). By taking the approximation of  $y^c = y(\alpha + \beta y)$ , in which  $\alpha$  and  $\beta$  can be estimated by using a least square method, Eqn. (A.1) is rewritten as:

$$\frac{dy}{dt} = a - by(\alpha + \beta y) \quad (\text{A.4})$$

$$\frac{dy}{dt} = (-b\beta)\left(-\frac{a}{b\beta} + \frac{\alpha}{\beta}y + y^2\right) \quad (\text{A.5})$$

Assuming  $A = -b\beta$ ,  $B = \frac{\alpha}{\beta}$  and  $C = \frac{-a}{b\beta} = \frac{a}{A}$ , integrating Eqn. (A.5) gives

$$\int_{y_0}^{y_t} \frac{1}{y^2 + By + C} dy = A \int_{t_0}^t dt \quad (\text{A.6})$$

If  $p_1$  and  $p_2$  are the two roots of the equation  $y^2 + By + C = 0$ , then

$$p_1 = \frac{-B + \sqrt{B^2 - 4C}}{2} \geq 0 \quad (\text{A.7})$$

$$p_2 = \frac{-B - \sqrt{B^2 - 4C}}{2} \leq 0 \quad (\text{A.8})$$

- When  $y_0 \geq p_1$  (i.e. for the flow recession period), the left side of Eqn. (A.6) is rewritten as:

$$\int_{y_0}^{y_t} \frac{1}{y^2 + By + C} dy = \int_{y_0}^{y_t} \left( \frac{1}{p_1 - p_2} \right) \left( \frac{1}{y - p_1} - \frac{1}{y - p_2} \right) dy \quad (\text{A.9})$$

The analytical solution to Eqn. (A.6) is therefore obtained by:

$$y_t = p_2 + (p_1 - p_2) \left[ 1 - A(p_1 - p_2)(t - t_0) \frac{y_0 - p_1}{y_0 - p_2} \right]^{-1} \quad (\text{A.10})$$

- When  $y_0 < p_1$  (i.e. for the flow rising period), similarly the analytical solution to Eqn. (A.6) is obtained by:

$$y_t = p_1 - (p_1 - p_2) \left[ 1 - A(p_1 - p_2)(t - t_0) \frac{y_0 - p_2}{p_1 - y_0} \right]^{-1} \quad (\text{A.11})$$

- (c)  $a \neq 0$ ,  $c > 2$  (e.g.  $c = 2.0 \sim 4.0$  for the subsurface flow equation in TOPKAPI). By taking the substitution of  $u = y^{-(c-1)}$ , Eqn. (A.1) is rewritten as:

$$\frac{du}{dt} = b(c-1) - a(c-1)u^{\frac{c}{c-1}} \quad (\text{A.12})$$

Since the term of  $\frac{c}{c-1}$  in Eqn. (A.12) falls in the range 1~2 now, its solution can be obtained analytically based on the approximation described above.



